DOI: 10.1002/ejic.200900904

Icosahedral Ga-Centred Nickel Carbonyl Clusters: Synthesis and Characterization of $[H_{3-n}Ni_{12}(\mu_{12}\text{-}Ga)(CO)_{22}]^{n-}$ (n = 2, 3) and $[Ni_{14.3}(\mu_{12}\text{-}Ga)(CO)_{24.3}]^{3-}$ Anions

Cristina Femoni,[a] Maria Carmela Iapalucci,*[a] Giuliano Longoni,[a] and Stefano Zacchini[a]

Keywords: Cluster compounds / Carbonyl ligands / Nickel / Gallium / Hydrides

The reaction of $[Ni_5(CO)_{12}]^{2-}$ or $[Ni_6(CO)_{12}]^{2-}$ with $GaCl_3$ in dichloromethane under a nitrogen atmosphere affords a mixture of $[Ni_{12+x}(\mu_{12}\text{-}Ga)(CO)_{22+x}]^{3-}$ (x = 0–3) clusters. Short exposure of the above mixture to a carbon monoxide atmosphere leads to the green icosahedral $[Ni_{12}(\mu_{12}\text{-}Ga)(CO)_{22}]^{3-}$ trianion, which was isolated and characterized as its $[NnBu_4]^+$ salt. In contrast, crystallization of the above mixture in the presence of $Ni(CO)_4$ enabled isolation of a cocrystallized mixture of $[Ni_{14}(\mu_{12}\text{-}Ga)(CO)_{24}]^{3-}$ (70%) and $[Ni_{15}(\mu_{12}\text{-}Ga)(CO)_{25}]^{3-}$ (30%). As inferable from its structure, the additional three Ni(CO) moieties condense onto interlayer faces of the icosahedron. Protonation of $[Ni_{12}(\mu_{12}\text{-}Ga)(CO)_{22}]^{3-}$ affords the corresponding $[HNi_{12}(\mu_{12}\text{-}Ga)(CO)_{22}]^{2-}$ hydride derivative, which was isolated in a pure state and fully characterized. All of the above compounds conform to the cluster-borane analogy, by the inclusion principle, and none exhibits relevant redox behaviour.

Introduction

Several metal carbonyl clusters adopting an icosahedral geometry are known. The great majority is based on a noncentred icosahedron having the 12 vertices constituted by 10 nickel metal atoms and a pair of *trans* main-group elements (E).[1–5] A few of them display 12 metal vertices and are centred by an interstitial E atom, for example, $[Ni_{12}(\mu_{12}\text{-}E)(CO)_{22}]^{2-}$ (E = Ge, Sn),[6] $[Rh_{12}(\mu_{12}\text{-}Sn)(CO)_{27}]^{4-}$[7] and $[Rh_{12}(\mu_{12}\text{-}Sb)(CO)_{27}]^{3-}$.[8] All formally feature 13 skeletal electron pairs, so fuelling through the inclusion principle[9] the cluster-borane analogy.[10] However, it was shown that $[Rh_{12}(\mu_{12}\text{-}Sn)(CO)_{27}]^{4-}$ can reversibly lose carbon monoxide to give the electron-poor $[Rh_{12}(\mu_{12}\text{-}Sn)(CO)_{26}]^{4-}$ and $[Rh_{12}(\mu_{12}\text{-}Sn)(CO)_{25}]^{4-}$ icosahedral clusters.[11] This exceptional behaviour probably descends from the fact that Rh and Sn belong to the same fifth period. Besides, the relatively low electronegativity of Sn could probably favour its shrinking to the point to fill a Rh_{12} icosahedron without need of swelling the cage. Indeed, under a rigid sphere model, the icosahedron would only allow lodging of a sphere having 95% of the size of the outer spheres. The above considerations were thought to impart a particular stability to the $Rh_{12}(\mu_{12}\text{-}Sn)$ metallic core. In partial agreement with the above reasoning, the $[Ni_{12}(\mu_{12}\text{-}Ge)(CO)_{22}]^{2-}$ dianion, which requires lodging in the icosahedral cavity of a smaller Ge atom, was reported to be less distorted and slightly more stable than the $[Ni_{12}(\mu_{12}\text{-}Sn)(CO)_{22}]^{2-}$ congener.[6]

In an attempt to implement such suggestions and eventually find new examples of icosahedral metal carbonyl clusters making exception to the cluster-borane analogy, we started an investigation of bimetallic Ni–Ga clusters, mainly on the basis of the consideration that Ga is comparable in size to Ge and features a minor Pauling electronegativity. These properties could eventually lead to undistorted icosahedral architectures and, consequently, to a more robust $[Ni_{12}(\mu_{12}\text{-}Ga)]$ metal core.

As a result, we report here a new series of icosahedral Ni carbonyl clusters, which represent the first examples of metal carbonyl clusters containing Ga as an interstitial element.[12]

Results and Discussion

Synthesis and Spectroscopic Characterization

The reaction of either $[Ni_5(CO)_{12}]^{2-}$ or $[Ni_6(CO)_{12}]^{2-}$ with $GaCl_3$ in dichloromethane under a nitrogen atmosphere leads to a mixture of $[Ni_{12+x}(\mu_{12}\text{-}Ga)(CO)_{22+x}]^{3-}$ (x = 0–3) trianions, formally according to Equation (1).

$$3[Ni_5(CO)_{12}]^{2-} + 4GaCl_3 \rightarrow [Ni_{12+x}(\mu_{12}\text{-}Ga)(CO)_{22+x}]^{3-} + (3-x)Ni(CO)_4 + (2-x)CO + 3[GaCl_4]^- \quad (1)$$

The presence of x = 0, 1, 2 and 3 derivatives is suggested by ESI-MS analysis of the mixture, as well as the ^1H NMR spectra of the protonated mixture, which display four major

[a] Dipartimento di Chimica Fisica ed Inorganica, Università di Bologna,
Viale Risorgimento 4, 40136 Bologna, Italy
Fax: +39-0512093690
E-mail: iapa@ms.fci.unibo.it

hydride signals. Owing to limited differential solubility in all solvents, the mixture could not be separated. However, the $[Ni_{12+x}(\mu_{12}\text{-}Ga)(CO)_{22+x}]^{3-}$ mixture is converted into pure $[Ni_{12}(\mu_{12}\text{-}Ga)(CO)_{22}]^{3-}$ trianion, according to Equation (2), by short exposure to a carbon monoxide atmosphere. The resulting green $[Ni_{12}(\mu_{12}\text{-}Ga)(CO)_{22}]^{3-}$ trianion was crystallized in its $[NnBu_4]^+$ salt by layering isopropyl alcohol on top of its dichloromethane solution. It shows infrared carbonyl absorptions in dichloromethane at 1999(s) and 1790(m) cm^{-1}.

$$[Ni_{12+x}(\mu_{12}\text{-}Ga)(CO)_{22+x}]^{3-} + 3xCO \leftrightarrows [Ni_{12}(\mu_{12}\text{-}Ga)(CO)_{22}]^{3-} + xNi(CO)_4 \quad (2)$$

Conversely, we only succeeded in isolating a cocrystallized mixture of $[Ni_{14}(\mu_{12}\text{-}Ga)(CO)_{24}]^{3-}$ and $[Ni_{15}(\mu_{12}\text{-}Ga)(CO)_{25}]^{3-}$ in a 70:30 ratio, by crystallization in dichloromethane/isopropyl alcohol of the $[NnBu_4]_3[Ni_{12+x}(\mu_{12}\text{-}Ga)(CO)_{22+x}]$ mixture in the presence of deliberately added $Ni(CO)_4$.

A first difference between the new $[Ni_{12}(\mu_{12}\text{-}Ga)(CO)_{22}]^{3-}$ cluster and the $[Ni_{12}(\mu_{12}\text{-}E)(CO)_{22}]^{2-}$ (E = Ge, Sn) congeners resides in its aptitude toward protonation to its corresponding hydride derivative. As shown by Equation (3), the protonation is reversible and the trianion is partially or completely regenerated by dissolving the hydride derivative in basic solvents such as DMF or DMSO.

$$[Ni_{12}(\mu_{12}\text{-}Ga)(CO)_{22}]^{3-} + H^+ \underset{THF}{\overset{DMSO}{\rightleftharpoons}} [HNi_{12}(\mu_{12}\text{-}Ga)(CO)_{22}]^{2-} \quad (3)$$

The $[HNi_{12}(\mu_{12}\text{-}Ga)(CO)_{22}]^{2-}$ dianion has been isolated in a pure state by crystallization of its $[NnBu_4]^+$ salt from acetone/isopropyl alcohol mixtures. It shows infrared carbonyl absorptions in acetone at 2025(s) and 1826(m) cm^{-1}. Its ^1H NMR spectrum (Figure 1) displays a signal at δ = –13.56 ppm, which corresponds to one of the hydride signals of the $[HNi_{12+x}(\mu_{12}\text{-}Ga)(CO)_{22+x}]^{2-}$ mixture.

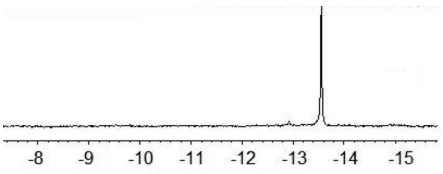

Figure 1. ^1H NMR spectrum of the $[HNi_{12}(\mu_{12}\text{-}Ga)(CO)_{22}]^{2-}$ dianion in $[D_6]$acetone.

The relatively enhanced stability of $[Ni_{12}(\mu_{12}\text{-}Ga)(CO)_{22}]^{3-}$ under carbon monoxide represents a second difference with $[Ni_{12}(\mu_{12}\text{-}Ge)(CO)_{22}]^{2-}$ and $[Ni_{12}(\mu_{12}\text{-}Sn)(CO)_{22}]^{2-}$. Indeed, the first of the two latter compounds promptly reacts with CO to give the stable pentagonal antiprismatic $[Ni_{10}(\mu_{10}\text{-}Ge)(CO)_{20}]^{2-}$ by loss of the apical Ni atoms, whereas the second is more extensively degraded to yet uncharacterized Ni–Sn species.[6] Conversely, $[Ni_{12}(\mu_{12}\text{-}Ga)(CO)_{22}]^{3-}$ is unaffected by short exposure to carbon monoxide at atmospheric pressure, although it is completely degraded by long exposures.

X-ray Structures of $[Ni_{12}(\mu_{12}\text{-}Ga)(CO)_{12}(\mu\text{-}CO)_6(\mu_3\text{-}CO)_4]^{3-}$, $[HNi_{12}(\mu_{12}\text{-}Ga)(CO)_{12}(\mu\text{-}CO)_8(\mu_3\text{-}CO)_2]^{2-}$ and $[Ni_{14.3}(\mu_{12}\text{-}Ga)(CO)_{24.3}]^{3-}$

$[NnBu_4]_3[Ni_{12}Ga(CO)_{22}]\cdot 2CH_2Cl_2$

The unit cell of $[NnBu_4]_3[Ni_{12}Ga(CO)_{22}]\cdot 2CH_2Cl_2$ contains 4 anions, 12 cations and 8 dichloromethane molecules separated by normal contacts. The structure of the $[Ni_{12}(\mu_{12}\text{-}Ga)(CO)_{12}(\mu\text{-}CO)_6(\mu_3\text{-}CO)_4]^{3-}$ trianion is shown in Figure 2; the adopted numbering scheme and the most significant bond lengths are collected in Table 1. Its metal framework may be described as a Ga-centred icosahedron of Ni atoms. Owing to a slight elongation along the pseudo C_5 axis passing through Ni2, Ga and Ni6, the metal framework is more precisely described as a bicapped pentagonal antiprism. It is likely that the above distortion is due to the CO ligands, which are layered in a 1-5-5-5-5-1 sequence of *terminal-bridge-terminal-terminal-bridge-terminal* CO groups describing a fused double icosahedron missing the shared vertex. As a result of the above sequence, there are no CO ligands spanning the interlayer edges or faces and shortening the bonding interlayer contacts between the two pentagonal rings of the inner Ni_{10} pentagonal antiprism. Indeed, six CO bridging ligands span three out of five edges of each pentagonal ring of the antiprism. Four carbonyl groups cap the triangular faces individuated by the remaining pentagonal edges and the apical Ni2 and Ni6 atoms. Finally, the CO ligand shell is completed by 12 terminal ligands, 1 per each Ni atom. As a whole, the carbonyl stereochemistry is very similar, though not identical, to the one displayed by the $[Ni_{12}(\mu_{12}\text{-}E)(CO)_{22}]^{2-}$ (E = Ge, Sn) congeners.[6]

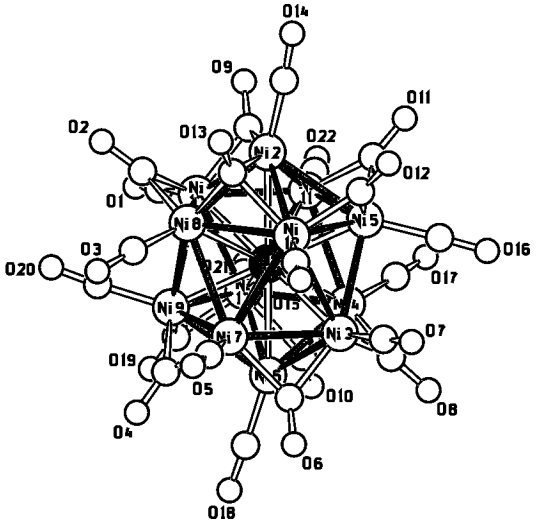

Figure 2. The structure of $[Ni_{12}(\mu_{12}\text{-}Ga)(CO)_{12}(\mu\text{-}CO)_6(\mu_3\text{-}CO)_4]^{3-}$.

Table 1. Range and average bond lengths [Å] in the title Ni–Ga clusters.

Distance	$[Ni_{12}(\mu_{12}\text{-}Ga)(CO)_{22}]^{3-}$	$[HNi_{12}(\mu_{12}\text{-}Ga)(CO)_{22}]^{2-}$	$[Ni_{14.3}(\mu_{12}\text{-}Ga)(CO)_{24.3}]^{3-}$
Ga–Ni range	2.4641(7)–2.6747(8)	2.4994(14)–2.6848(15)	2.4547(7)–2.6082(7)
Average	2.524	2.542	2.532
Ni–Ni icosahedron range	2.4762(8)–2.8564(9)	2.509(2)–2.884(2)	2.4634(7)–2.8393(8)
Average	2.653	2.656	2.643
Caps range	–	–	2.4384(7)–2.7351(7)
Average	–	–	2.502
Ni–C terminal range	1.767(5)–1.785(5)	1.736(15)–1.782(14)	1.754(7)–1.794(4)
Average	1.778	1.757	1.776
Edge-bridging range	1.888(5)–1.924(5)	1.889(14)–2.034(13)	1.84(3)–2.25(3)
Average	1.902	1.925	1.918
Face-bridging range	1.923(5)–2.083(5)	1.939(13)–2.098(13)	–
Average	2.000	2.023	–
C–O range	1.133(6)–1.189(5)	1.121(15)–1.182(13)	1.128(5)–1.184(5)
Average	terminal 1.141 edge-bridging1.168 face-bridging 1.183	terminal 1.146 edge-bridging 1.158 face-bridging 1.182	terminal 1.139 edge-bridging 1.167

[NnBu$_4$]$_2$[HNi$_{12}$Ga(CO)$_{22}$]

The unit cell contains one $[HNi_{12}(\mu_{12}\text{-}Ga)(CO)_{12}(\mu\text{-}CO)_8(\mu_3\text{-}CO)_2]^{2-}$ dianion and two $[N\textit{n}Bu_4]^+$ cations, whereas in the asymmetric unit only one half of the cluster and one cation are present, as the Ga atom lies on the crystallographic centre of symmetry. The structure of the dianion is reported in Figure 3; the adopted numbering scheme and the most relevant bonding interactions are collected in Table 1. As a whole, the structure is very similar to that of the parent trianion, the only difference being represented by a lengthening of the Ni7–C2 contact [2.213(14) Å] beyond the usual bond length. Owing to that, the C2–O2 carbonyl has been somehow arbitrarily shown as edge-bridging in Figure 3.

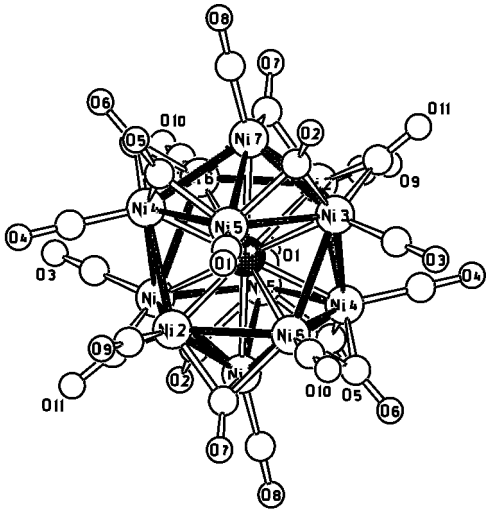

Figure 3. The structure of $[HNi_{12}(\mu_{12}\text{-}Ga)(CO)_{12}(\mu\text{-}CO)_8(\mu_3\text{-}CO)_2]^{2-}$.

This slight change is probably a consequence of the reduced negative charge of the anion, which decreases the need of back-donation from the $Ni_{12}Ga$ core towards the CO ligand shell. A second difference is present in the individual Ni–Ga and Ni–Ni bond contacts. In general, on reducing the negative charge of the anion one should expect a slight shrinking of the metal core. However, examination of Table 1 argues against it and points out that the metal core of $[HNi_{12}(\mu_{12}\text{-}Ga)(CO)_{12}(\mu\text{-}CO)_8(\mu_3\text{-}CO)_2]^{2-}$ undergoes a slight swelling with respect to that of the parent trianion. In particular there is a small but significant elongation of the Ni2–Ni5 and Ni5–Ni6 edges (which have been arbitrarily omitted in Figure 3) and the Ni2–Ni6 bond.

It seemed reasonable that the hydride hydrogen atom could be located and disordered over the above two crystallographically equivalent faces or edges. Theoretical calculations with Xhydex[13] were carried out. The preliminary output resulted in three possible face-bridging hydrides with similar potential energy, respectively located on the Ni2–Ni5–Ni6, Ni3–Ni4–Ni6 and Ni3–Ni5–Ni6 faces and equally disordered on their correspondent centrosymmetric images. However, after refinement, only the hydride atom on the Ni2–Ni5–Ni6 face remained stable and displayed Ni–H bond lengths in the 1.70–2.06 Å range of values. As expected, the preferred hydride position is where the longest Ni–Ni bond lengths [Ni3–Ni6 2.820(2) and Ni5–Ni6 2.884(2) Å] are found.

[NnBu$_4$]$_3$[Ni$_{14.3}$Ga(CO)$_{24.3}$]·2CH$_2$Cl$_2$

The unit cell of $[N\textit{n}Bu_4]_3[Ni_{14.3}Ga(CO)_{24.3}]\cdot 2CH_2Cl_2$ contains 4 anions, 12 cations and 8 dichloromethane molecules separated by normal contacts. The structure of the $[Ni_{14.3}Ga(CO)_{24.3}]^{3-}$ trianion is shown in Figure 4; the most relevant bonding contacts are collected in Table 1. The central core of the cluster anion is again a distorted icosahedron slightly elongated along both the Ni3–Ga–Ni8 and Ni2–Ga–Ni6 axes. The icosahedron is capped by three Ni(CO) moieties on two contiguous (Ni7 and Ni12) and one opposite (Ni16) interlayer triangular faces. However, the third cap, namely, Ni16–CO25, shows a refined occupancy fraction of 0.29, arising from the presence in the crystals of both $[Ni_{14}(\mu_{12}\text{-}Ga)(CO)_{24}]^{3-}$ (ca. 70%) and $[Ni_{15}(\mu_{12}\text{-}Ga)(CO)_{25}]^{3-}$ (ca. 30%) trianions. This disorder justifies the given fractional composition. Moreover, the presence of Ni(CO) moieties binding two interlayer Ni_5 rings opposes the deformation shown by both $[Ni_{12}Ga(CO)_{22}]^{3-}$ and

$[HNi_{12}Ga(CO)_{22}]^{2-}$. As a result, the average Ni–Ni distance of the icosahedral moiety is the shortest of this series of compounds (see Table 1).

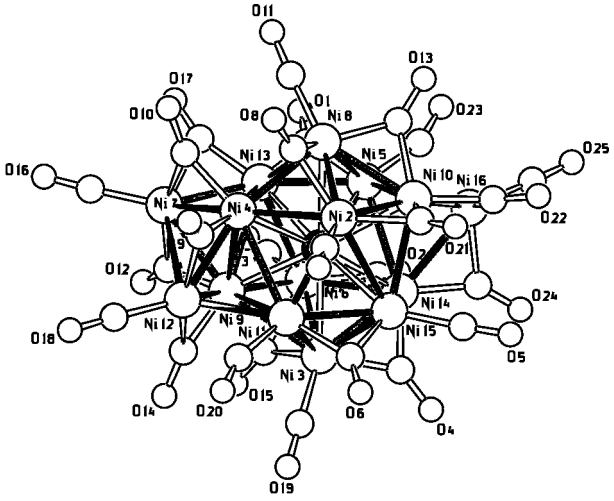

Figure 4. Structure of $[Ni_{12+x}(\mu_{12}\text{-}Ga)(CO)_{22+x}]^{3-}$ [x = 2 (70%), 3 (30%) based on occupancy fraction of Ni16 and CO25, which refines to ca. 0.3].

As a further difference, no more symmetrical face bridging carbonyl groups are present, even if five carbonyl groups (represented as edge-bridging in Figure 4) lean toward a third Ni atom and display contacts shorter than the sum of their van der Waals radii [namely, Ni12–C20 2.203(4), Ni4–C8 2.322(4), Ni5–C13 2.433(5), Ni9–C1 2.272(4) and Ni15–C4 2.434(4) Å].

Finally, the two contiguous caps reciprocally interact, as inferable by a bonding contact of 3.074 Å, whereas the Ni–Ni interactions between the caps and the Ni atoms of the inner icosahedral core are in the range 2.4384(7)–2.4724(7) Å. Though weak, the above additional interaction probably favours such contiguity, rather than the capping of nonadjacent faces. Conversely, the subsequent addition of a third contiguous Ni(CO) cap is likely disfavoured by the unavoidable crowding of the carbonyl ligands.

EHMO Calculations and Redox Behaviour of $[Ni_{12}(\mu_{12}\text{-}Ga)(CO)_{22}]^{3-}$

According to the EHMO (extended Hückel molecular orbital) method, the frontier region of $[Ni_{12}(\mu_{12}\text{-}Ga)(CO)_{22}]^{3-}$ (see Figure 5) displays a pair of quasi degenerate filled molecular orbitals as HOMO, which fall almost in the middle of a wide gap of ca. 1.6 eV between the LUMO and the third HOMO. The stabilization of the above two MOs is due to the bonding character of the interaction between the p_x and p_y atomic orbitals (AOs) of Ga with one or a pair of contiguous Ni atoms belonging to the two pentagonal faces of the inner antiprism (see bottom part of Figure 5). All other Ni–Ga and Ni–Ni contributions are either weakly bonding or nonbonding, whereas the C–O interactions are mainly antibonding. In particular, the interaction of the apical Ni atoms (Ni2 and Ni6 of Figure 2) with Ga 4p AOs is antibonding. As a result, these interactions feature the least Ni–Ga overlap population, in agreement with the slight elongation of the icosahedron along the Ni2–Ga–Ni6 axis. Practically identical features are also shown by the previously reported $[Ni_{12}(\mu_{12}\text{-}Ge)(CO)_{22}]^{2-}$ and $[Ni_{12}(\mu_{12}\text{-}Sn)(CO)_{22}]^{2-}$, which are both isoelectronic and isostructural. In contrast, EHMO simulations of hypothetical $[Ni_{12}(\mu_{12}\text{-}E)(CO)_{22}]^{n-}$ (E = Sb or Bi, n = 1; E = Se or Te, n = 0) isoelectronic and isostructural clusters suggest that interstitial group 15 and 16 elements should only feature a wide HOMO–LUMO gap of ca. 1.6–1.8 eV.

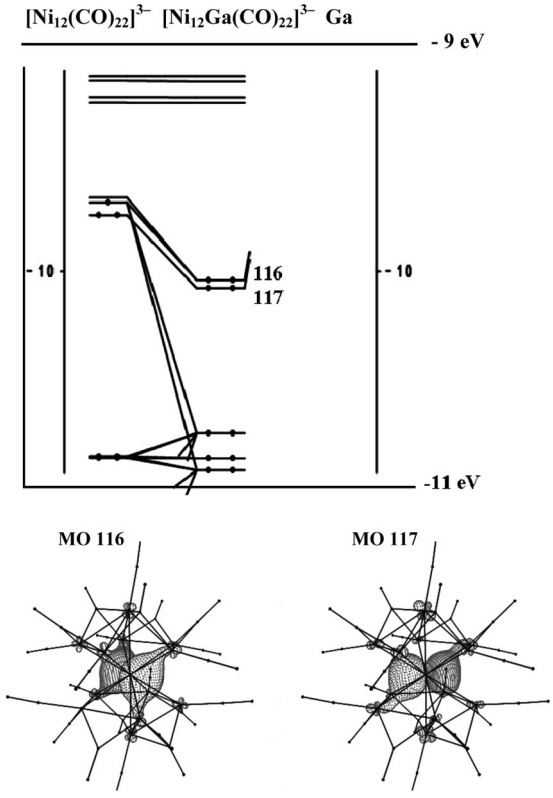

Figure 5. Frontier region of the EHMO diagram (top) calculated with CACAO[14] and picture of the quasidegenerate 116 and 117 HOMOs of $[Ni_{12}Ga(CO)_{22}]^{3-}$ (bottom).

The presence of a pair of quasidegenerate filled MOs as HOMO, falling almost in the middle of a wide gap, is also displayed by the Ni-centred $[Ni_{11}(\mu_6\text{-}E)_2(CO)_{18}]^{4-}$ (E = Sb, Bi)[15,16] and $[Ni_{13}(\mu_7\text{-}Sb)_2(CO)_{24}]^{4-}$ multivalent clusters.[17,18] Both display two reversible oxidations and the resulting tri- and dianions are even more easily workable than the corresponding tetraanions.

In spite of the similarities between the EHMO diagrams of E-centred $[Ni_{12}(\mu_{12}\text{-}Ga)(CO)_{22}]^{3-}$ and Ni-centred $[Ni_{11}(\mu_6\text{-}E)_2(CO)_{18}]^{4-}$ (E = Sb, Bi),[15,16] the cyclic voltammetry of the former species only discloses irreversible redox changes. In particular, at the highest scan rate (1 V s^{-1}), it shows two well-defined oxidation steps at +0.75 and +1.26 V (vs. SCE), accompanied in the back scan by ill-reproducible and less-intense reduction signals at ca. +1.0 and +0.4 V. Upon a decrease in the scan rate to 0.1 and 0.01 V s^{-1} the back waves become almost unnoticeable.

Concluding Remarks

The calculated average radius of the interstitial Ga atoms in the title icosahedral compounds is comprised in the narrow 1.20–1.21 Å range of values, which is very close to the accepted covalent radius of Ga (1.22 Å)[19] and corresponds to ca. 91% of the radii of the surrounding Ni atoms. Therefore, both steric and electronic (viz. the above EHMO diagram) factors seemed favourable but turned out to be not sufficient to grant multivalence, as well as stability in a different ligand shell, to the $[Ni_{12}(\mu_{12}\text{-}Ga)(CO)_{22}]^{3-}$ icosahedral cluster, as it instead occurs for $[Ni_{11}(\mu_6\text{-}E)_2(CO)_{18}]^{4-}$ (E = Sb, Bi) and $[Rh_{12}(\mu_{12}\text{-}Sn)(CO)_{25}]^{4-}$.

The difference between Ni-centred and E-centred Ni clusters is particularly striking. In spite of their different compositions, the two architectures feature identical numbers of Ni–Ni (30, dotted bonds in Figure 6) and Ni–E (12, blackened bonds) interactions and similar EHMO diagrams. The only noticeable difference between the two architectures in EHMO calculations is represented by a significant increase in the average overlap population (OP) of Ni–E bonds, on going from group 13 or 14 (OP ca. 0.2) to group 15 (OP ca. 0.3) elements. Besides, in all cases, the umbrella sticks of geometry **A** in Figure 6 show ca. 45% of the rib's OP, whereas the opposite trend is observed in **B**.

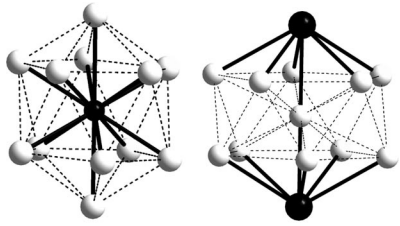

Figure 6. Schematic structure of $[Ni_{12}(\mu_{12}\text{-}E)(CO)_{22}]^{n-}$ and $[Ni_{11}(\mu_6\text{-}E)_2(CO)_{18}]^{n-}$ (E as black spheres), pointing out the Ni–E bonds acting as sticks and ribs of the two differently oriented (head–head in **A** and tail–tail in **B**) $Ni_6(\mu_6\text{-}E)$ umbrella.

Such a trend formally explains the greater reactivity of $[Ni_{12}(\mu_{12}\text{-}E)(CO)_{22}]^{n-}$ species under a CO atmosphere in comparison with $[Ni_{11}(\mu_6\text{-}E)_2(CO)_{18}]^{n-}$. In particular, $[Ni_{12}(\mu_{12}\text{-}Ge)(CO)_{22}]^{2-}$ is quantitatively degraded by CO at atmospheric pressure to a pentagonal antiprismatic $[Ni_{10}(\mu_{10}\text{-}Ge)(CO)_{20}]^{2-}$.[6] It may therefore be speculated that the trend of Ni–E OP and the opposite orientation of their umbrella concur in tightening geometry **B** and explain the different stability of the above geometries also upon a redox change.

Experimental Section

General: All reactions and sample manipulations were carried out by using standard Schlenk techniques under a nitrogen atmosphere and in dried solvents. The $[Ni_6(CO)_{12}]^{2-}$ salts were prepared according to literature methods.[20] Analysis of Ni were performed by atomic absorption on a Pye-Unicam instrument. Analyses of C, H and N were obtained with a ThermoQuest FlashEA 1112NC instrument. IR spectra were recorded with a Perkin–Elmer SpectrumOne interferometer in CaF_2 cells. ^1H NMR spectra were recorded with a Varian Mercury 400 MHz spectrometer, and referenced to internal TMS. The structure figures were drawn with SCHAKAL99.[21] EHMO calculations have been carried out with CACAO.[14]

$[NnBu_4]_3[Ni_{14.3}Ga(CO)_{24.3}]$: A solution of $GaCl_3$ (0.37 g, 2.10 mmol) in dichloromethane (20 mL) was added in portions to $[NnBu_4]_2[Ni_6(CO)_{12}]$ (1.85 g, 1.58 mmol) dissolved in dichloromethane (50 mL) with stirring. The mixture was left to react for 24 h, until IR monitoring showed disappearance of $[Ni_6(CO)_{12}]^{2-}$ from solution. The resulting dark-brown suspension was evaporated to dryness and washed with water (3×15 mL) and isopropyl alcohol (2×20 mL). The residual brown material was extracted in dichloromethane (20 mL) and $Ni(CO)_4$ (0.2 mL) was added. Precipitation by slow diffusion of isopropyl alcohol (60 mL) gave dark-brown crystals of $[NnBu_4]_3[Ni_{14.3}Ga(CO)_{24.3}]\cdot 2CH_2Cl_2$ (yield 0.654 g, 39.7% based on Ni). The salt is soluble in CH_2Cl_2, THF, acetone, acetonitrile, DMF and DMSO, sparingly soluble in alcohols and insoluble in nonpolar solvents. IR (CH_2Cl_2): $\tilde{\nu}_{CO}$ = 2009 (s), 1879 (m, br.), 1822 (sh.) cm^{-1}. $[NnBu_4]_3[Ni_{14.3}Ga(CO)_{24.3}]\cdot 2CH_2Cl_2$: calcd. Ni 33.76, C 35.89, H 4.51, N 1.69; found Ni 33.89, C 35.71, H 4.46, N 1.71.

$[NnBu_4]_3[Ni_{12}Ga(CO)_{22}]$: Solid $[NnBu_4]_3[Ni_{14.3}Ga(CO)_{24.3}]$ (0.521 g, 0.21 mmol) was dissolved in dichloromethane (30 mL) in a 200-mL flask and stirred under a static carbon monoxide atmosphere. The initial dark red-brown colour of the solution slowly turned green-brown. The resulting solution was evaporated to dryness to eliminate $Ni(CO)_4$, and the residue was dissolved in dichloromethane (15 mL). Precipitation by diffusion of isopropyl alcohol (30 mL) gave $[NnBu_4]_3[Ni_{12}Ga(CO)_{22}]\cdot 2CH_2Cl_2$ within a few days as brown crystals (0.39 g, 68.2% based on Ni). The salt is soluble in CH_2Cl_2, THF, acetone, acetonitrile, DMF and DMSO, sparingly soluble or insoluble in alcohols and insoluble in nonpolar solvents. IR (CH_2Cl_2): $\tilde{\nu}_{CO}$ = 1999 (s), 1790 (m) cm^{-1}. $[NnBu_4]_3[Ni_{12}Ga(CO)_{22}]\cdot 2CH_2Cl_2$: calcd. Ni 30.78, C 37.80, H 4.89, N 1.84; found Ni 30.91, C 37.73, H 4.72, N 1.82.

$[NnBu_4]_2[HNi_{12}Ga(CO)_{22}]$: Solid $[NnBu_4]_3[Ni_{12}Ga(CO)_{22}]\cdot 2CH_2Cl_2$ (0.32 g, 0.14 mmol) was dissolved in THF and treated dropwise whilst stirring with a solution of dilute acid (1 mL of 20% H_2SO_4 in 5 mL of THF) monitoring the reaction by IR spectroscopy. The resulting brown solution was evaporated under vacuum. The precipitate was washed several times with water and dried. The residue was extracted in acetone (10 mL) and precipitated by diffusion of isopropyl alcohol (20 mL) to obtain black crystals of $[NnBu_4]_2[HNi_{12}Ga(CO)_{22}]$ (0.28 g). The salt is soluble in CH_2Cl_2, THF, acetone, acetonitrile, DMF and DMSO and insoluble in nonpolar solvents. The compound is deprotonated to $[Ni_{12}Ga(CO)_{22}]^{3-}$ both in DMF and DMSO. ^1H NMR ([D$_6$]acetone, 293 K): δ = –13.5 ppm. IR (acetone): $\tilde{\nu}_{CO}$ = 2025 (s), 1826 (m) cm^{-1}. $[NnBu_4][HNi_{12}Ga(CO)_{22}]$: calcd. Ni 37.53, C 34.56, H 3.89, N 1.49; found Ni 37.46, C 34.49, H 3.91, N 1.47.

X-ray Crystallographic Studies: Crystal data and collection details for $[NnBu_4]_3[Ni_{12}Ga(CO)_{22}]\cdot 2CH_2Cl_2$, $[NnBu_4]_2[HNi_{12}Ga(CO)_{22}]$ and $[NnBu_4]_3[Ni_{14.3}Ga(CO)_{24.3}]\cdot 2CH_2Cl_2$ are reported in Table 2. The diffraction experiments were carried out with a Bruker APEX II diffractometer equipped with a CCD detector by using Mo-K_α radiation. Data were corrected for Lorentz polarization and absorption effects (empirical absorption correction SADABS).[22] Structures were solved by direct methods and refined by full-matrix least-squares based on all data using F^2.[23] Hydrogen atoms were fixed at calculated positions and refined by a riding model. All

Table 2. Crystal data and experimental details for $[NnBu_4]_3[Ni_{12}Ga(CO)_{22}]\cdot 2CH_2Cl_2$, $[NnBu_4]_2[HNi_{12}Ga(CO)_{22}]$ and $[NnBu_4]_3[Ni_{14.3}Ga(CO)_{24.3}]\cdot 2CH_2Cl_2$.

	$[NnBu_4]_3[Ni_{12}Ga(CO)_{22}]\cdot 2CH_2Cl_2$	$[NnBu_4]_2[HNi_{12}Ga(CO)_{22}]$	$[NnBu_4]_3[Ni_{14.3}Ga(CO)_{24.3}]\cdot 2CH_2Cl_2$
Formula	$C_{72}H_{112}Cl_4GaN_3Ni_{12}O_{22}$	$C_{54}H_{72}GaN_2Ni_{12}O_{22}$	$C_{74.29}H_{112}Cl_4GaN_3Ni_{14.29}O_{24.29}$
Fw	2287.69	1875.38	2486.06
T [K]	100(2)	296(2)	100(2)
λ [Å]	0.71073	0.71073	0.71073
Crystal system	monoclinic	triclinic	monoclinic
Space group	$P2_1/n$	$P\bar{1}$	$P2_1/n$
a [Å]	18.6475(15)	11.241(2)	13.3235(14)
b [Å]	21.3024(18)	13.908(3)	33.238(4)
c [Å]	23.3035(19)	14.287(3)	21.338(2)
α [°]	90	61.497(2)	90
β [°]	99.8230(10)	68.815(2)	93.022(2)
γ [°]	90	68.798(2)	90
Cell Volume [Å^3]	9121.3(13)	1780.8(6)	9436.3(17)
Z	4	1	4
$D_{calcd.}$ [g cm^{-3}]	1.666	1.749	1.750
μ [mm^{-1}]	2.887	3.530	3.238
F(000)	4704	953	5088
Crystal size [mm]	$0.21\times0.14\times0.11$	$0.15\times0.10\times0.08$	$0.22\times0.14\times0.11$
θ limits [°]	1.46–26.00	1.67–25.00	1.55–27.00
Index ranges	$-23 \le h \le 23$	$-13 \le h \le 13$	$-17 \le h \le 17$
	$-26 \le k \le 26$	$-16 \le k \le 16$	$-42 \le k \le 42$
	$-28 \le l \le 28$	$-16 \le l \le 16$	$-27 \le l \le 27$
Reflections collected	92429	17002	103831
Independent reflections	17895 [R_{int} = 0.0555]	6251 [R_{int} = 0.0952]	20591 [R_{int} = 0.0725]
Completeness to θ = 25.03°	99.9	99.7	100.0
Data/restraints/parameters	17895/440/1055	6251/174/412	20591/365/1191
Goodness on fit on F^2	1.086	0.968	1.030
R_1 [$I>2\sigma(I)$]	0.0368	0.0714	0.0365
wR_2 (all data)	0.1064	0.2100	0.0852
Largest diff. peak/hole [e Å^{-3}]	0.957/–0.783	1.240/–0.479	0.987/–0.752

non-hydrogen atoms were refined with anisotropic displacement parameters, unless otherwise stated.

$[NnBu_4]_3[Ni_{12}Ga(CO)_{22}]\cdot 2CH_2Cl_2$: The asymmetric unit contains one cluster anion, three $[NnBu_4]^+$ cations and two CH_2Cl_2 molecules all located in general positions. One of the two CH_2Cl_2 molecules appears to be disordered; its atoms have been split into two positions and refined isotropically with one independent occupancy factor. Similar U restraints were applied to the C (s.u. 0.003), O and Cl (s.u. 0.005) atoms. Restraints to bond lengths were applied as follow (s.u. 0.01): 1.47 Å for C–N and 1.53 Å in $[NnBu_4]^+$; 1.75 Å for C–Cl in CH_2Cl_2.

$[NnBu_4]_2[HNi_{12}Ga(CO)_{22}]$: The asymmetric unit contains one half of the cluster anion and one $[NnBu_4]^+$ cation; the rest of the unit cell can be generated thanks to the centre of symmetry, located on the Ga atom. Similar U restraints were applied to the CO ligands and the cation (s.u. 0.01). Distance restraints of 1.54 Å (s.u. 0.02) were also applied to C–C bonds in the latter.

$[NnBu_4]_3[Ni_{14.3}Ga(CO)_{24.3}]\cdot 2CH_2Cl_2$: The asymmetric unit contains one cluster anion, three $[NnBu_4]^+$ cations and two CH_2Cl_2 molecules all located in general positions. One of the two CH_2Cl_2 molecules appears to be disordered; its atoms have been split into two positions and refined isotropically with one independent occupancy factor. The Ni16–C25–O25 group capping a triangular face of the icosahedral cage has a partial occupancy factor (0.2926 after refinement); in order to improve the model, also the three bridging carbonyls C22–O22, C23–O23 and C24–O24 have been split into two positions and refined with the same free variable of Ni16–C25–O25. Similar U restraints (s.u. 0.005) were applied to the C, O and Cl atoms. Restraints to bond lengths were applied as follow (s.u. 0.01): 1.47 Å for C–N and 1.53 Å in $[NnBu_4]^+$; 1.75 Å for C–Cl in CH_2Cl_2.

CCDC-741742 (for $[NnBu_4]_2[HNi_{12}Ga(CO)_{22}]$), -741743 (for $[NnBu_4]_3[Ni_{12}Ga(CO)_{22}]\cdot 2CH_2Cl_2$) and -741744 (for $[NnBu_4]_3[Ni_{14.3}Ga(CO)_{24.3}]\cdot 2CH_2Cl_2$) contain the supplementary crystallographic data for this paper. These data can be obtained free of charge from The Cambridge Crystallographic Data Centre via www.ccdc.cam.ac.uk/data_request/cif.

Acknowledgments

We wish to thank the University of Bologna (CLUSTERCAT) and Ministero dell'Università e della Ricerca (PRIN) for financial assistance.

[1] D. F. Rieck, J. A. Gavney, R. L. Norman, R. K. Hayashi, L. F. Dahl, *J. Am. Chem. Soc.* **1992**, *114*, 10369–10379.
[2] D. F. Rieck, R. A. Montag, T. S. McKechnie, L. F. Dahl, *J. Am. Chem. Soc.* **1986**, *108*, 1330–1331.
[3] R. E. Des Enfants II, J. A. Gavney, R. K. Hayashi, A. D. Rae, L. F. Dahl, A. Bjarnason, *J. Organomet. Chem.* **1990**, *383*, 543–572.
[4] P. D. Mlynek, L. F. Dahl, *Organometallics* **1997**, *16*, 1641–1654.
[5] A. J. Kahaian, J. B. Thoden, L. F. Dahl, *J. Chem. Soc., Chem. Commun.* **1992**, 353–355.
[6] A. Ceriotti, F. Demartin, B. T. Heaton, P. Ingallina, G. Longoni, M. Manassero, M. Marchionna, N. Masciocchi, *J. Chem. Soc., Chem. Commun.* **1989**, 786–787.
[7] C. Femoni, M. C. Iapalucci, G. Longoni, C. Tiozzo, S. Zacchini, B. T. Heaton, J. A. Iggo, *Dalton Trans.* **2007**, *35*, 3914–3923.

[8] J. L. Vidal, J. M. Troup, *J. Organomet. Chem.* **1981**, *213*, 351–363.
[9] J.-F. Halet, D. G. Evans, D. M. P. Mingos, *J. Am. Chem. Soc.* **1988**, *110*, 87–90.
[10] K. Wade, *Adv. Inorg. Chem. Radiochem.* **1976**, *18*, 1–66.
[11] C. Femoni, M. C. Iapalucci, G. Longoni, C. Tiozzo, S. Zacchini, B. T. Heaton, J. A. Iggo, P. Zanello, S. Fedi, M. V. Garland, C. Li, *Dalton Trans.* **2009**, 2217–2223.
[12] C. Femoni, M. C. Iapalucci, F. Kaswalder, G. Longoni, S. Zacchini, *Coord. Chem. Rev.* **2006**, *250*, 1580–1604.
[13] A. G. Orpen, *J. Chem. Soc., Dalton Trans.* **1980**, *12*, 2509–2516.
[14] C. Mealli, D. M. Proserpio, *J. Chem. Educ.* **1990**, *67*, 399–402.
[15] V. G. Albano, F. Demartin, C. Femoni, M. C. Iapalucci, G. Longoni, M. Monari, P. Zanello, *J. Organomet. Chem.* **2000**, *593–594*, 325–334.
[16] V. G. Albano, F. Demartin, M. C. Iapalucci, G. Longoni, M. Monari, P. Zanello, *J. Chem. Soc., Dalton Trans.* **1992**, *3*, 497–502.
[17] V. G. Albano, F. Demartin, M. C. Iapalucci, G. Longoni, A. Sironi, V. Zanotti, *J. Chem. Soc., Chem. Commun.* **1990**, 547–548.
[18] V. G. Albano, F. Demartin, M. C. Iapalucci, F. Laschi, G. Longoni, A. Sironi, P. Zanello, *J. Chem. Soc., Dalton Trans.* **1991**, 739–747.
[19] B. Cordero, V. Gómez, A. E. Platero-Prats, M. Revés, J. Echeverría, E. Cremades, F. Barragán, S. Alvarez, *Dalton Trans.* **2008**, 2832–2838.
[20] A. Ceriotti, G. Longoni, G. Piva, *Inorg. Synth.* **1988**, *26*, 312–315.
[21] E. Keller, *Schakal 99*, University of Freiburg, Germany, **1999**.
[22] G. M. Sheldrick, *SADABS*, University of Göttingen, Germany, **1996**.
[23] G. M. Sheldrick, *SHELX97*, University of Göttingen, Germany, **1997**.

Received: September 11, 2009
Published Online: January 19, 2010

